HHS Public Access

Author manuscript

Nat Med. Author manuscript; available in PMC 2014 March 01.

Published in final edited form as:

Nat Med. 2013 September ; 19(9): 1153–1156. doi:10.1038/nm.3250.

FGF21 contributes to neuroendocrine control of female reproduction

Bryn M. Owen[1], **Angie L. Bookout**[1,2], **Xunshan Ding**[3], **Vicky Y. Lin**[1], **Stan D. Atkin**[1], **Laurent Gautron**[2], **Steven A. Kliewer**[1,3,*], and **David J. Mangelsdorf**[1,4,*]

[1]Department of Pharmacology, University of Texas Southwestern Medical Center, Dallas TX 75390 USA

[2]Division of Hypothalamic Research, Department of Internal Medicine, University of Texas Southwestern Medical Center, Dallas TX 75390 USA

[3]Department of Molecular Biology, University of Texas Southwestern Medical Center, Dallas TX 75390 USA

[4]Howard Hughes Medical Institute, University of Texas Southwestern Medical Center, Dallas TX 75390 USA

Abstract

Preventing reproduction during nutritional deprivation is an adaptive process that is conserved and essential for the survival of species. In mammals, the mechanisms that inhibit pregnancy during starvation are complex and incompletely understood[1–7]. Here we show that exposure of female mice to FGF21, a fasting-induced hepatokine, mimics infertility secondary to starvation. Mechanistically, FGF21 acts on the suprachiasmatic nucleus (SCN) in the hypothalamus to suppress the vasopressin-kisspeptin signaling cascade, thereby inhibiting the proestrus surge in luteinizing hormone. Mice lacking the FGF21 co-receptor, β-Klotho, in the SCN are refractory to the inhibitory effect of FGF21 on female fertility. Thus, FGF21 defines an important liver-neuroendocrine axis that modulates female reproduction in response to nutritional challenge.

Fibroblast growth factor 21 (FGF21) is an atypical member of the FGF super-family that can enter the circulation and function as a hormone [8]. Physiologically, plasma FGF21 levels are increased during starvation as a result of hepatic PPARα-mediated gene transcription [9,10]. FGF21 coordinates a systemic response to fasting by increasing ketogenesis, suppressing growth, and promoting torpor [9,11–13]. Pharmacologically, FGF21 has beneficial metabolic effects in obese and diabetic animal models as an insulin sensitizer [12] and therefore considerable effort is being devoted to understanding its mechanism of action [14].

*To whom correspondence should be addressed. steven.kliewer@utsouthwestern.edu; davo.mango@utsouthwestern.edu.

Author Contributions

B.M.O. designed and performed all experiments, analyzed data and wrote the paper. A.L.B. generated *Klb*$^{tm1(Camk2a)}$::Tg(Fgf21) and *Klb*$^{tm1(Phox2b)}$::Tg(Fgf21) mice and designed and performed experiments. X.D. generated *Klb*^{tm1} mice. V.Y.L., S.A. and L.G. performed experiments and analyzed data. D.J.M. and S.A.K. supervised the project and wrote the paper.

We previously reported that transgenic (Tg) overexpression of FGF21 causes infertility in Tg(Fgf21) female but not male mice [9]. While the female Tg(Fgf21) mice are smaller and have higher insulin sensitivity, their body fat percentage, plasma adiponectin and plasma leptin concentrations do not differ from their wild-type counterparts[15]. Initial characterization of the cause of infertility revealed a delay in the onset of puberty (Fig. 1a) and a failure to mate with proven stud males (Fig. 1b). Vaginal cytology and ovarian histology demonstrated abnormalities consistent with anovulatory hypogonadism. Tg(Fgf21) mice rarely entered the ovulatory estrus phase of the cycle and displayed a prolonged diestrus (Fig. 1c). Ovarian histology revealed the presence of mature follicles in Tg(Fgf21) mice but there were few, if any, post-ovulation corpora lutea (Fig. 1d). The abnormal estrous cycles in female Tg(Fgf21) mice were concordant with altered plasma gonadotropin concentrations: while plasma follicle stimulating hormone (FSH) concentrations were normal, the levels of ovulation-inducing luteinizing hormone (LH) were lowered significantly compared to wild-type mice (Fig. 1e). These analyses demonstrate that female Tg(Fgf21) mice exhibit hypogonadotropic hypogonadism.

To assess the function of the hypothalamic-pituitary-gonadal axis in female Tg(Fgf21) mice, we performed a series of hormone challenge tests. In response to exogenous gonadotropin (PMSG), plasma estradiol levels increased normally in both wild-type and Tg(Fgf21) mice (Fig. 2a). However, ovariectomized Tg(Fgf21) mice had a markedly perturbed LH surge in response to exogenously administered estradiol compared to wild-type mice (Fig. 2b), suggesting a defect at the level of the hypothalamus or pituitary. When stimulated with a synthetic gonadotropin releasing hormone (GnRH)-receptor agonist (leuprolide), the pituitary of Tg(Fgf21) mice produced an LH surge of similar magnitude to that of wild-type mice (Fig. 2c). Therefore, the hypothalamus of Tg(Fgf21) mice fails to elicit an appropriate GnRH signal to the pituitary in response to a surge of estradiol. Consistent with this interpretation, transplantation of Tg(Fgf21) ovaries into wild-type recipients was sufficient to rescue ovarian function (Supplementary Fig. 1).

The LH surge is controlled by a hypothalamic neuroendocrine axis [16]. Kisspeptin, the product of the *Kiss1* gene, is expressed in the arcuate (Arc) and anteroventral periventricular (AVPV) nuclei of the hypothalamus, where it communicates changes in plasma estradiol to GnRH-neurons that, in turn, regulate pituitary gonadotropin secretion [17]. Upstream, the SCN plays an essential role in ovulation by communicating, via vasopressinergic neurons, to the kisspeptin axis in the AVPV and gating the LH surge [18,19]. In the Arc, a nucleus that mediates negative feedback effects of sex steroids on gonadotropin release[20], *Kiss1* gene expression was similar in female wild-type and Tg(Fgf21) mice (Fig. 2d). However, in the AVPV, where kisspeptin exerts positive feedback effects of estradiol and stimulates the pre-ovulatory LH surge[20], *Kiss1* gene expression was significantly lower in female Tg(Fgf21) mice compared to wild-type mice (Fig. 2d). Likewise, vasopressin (*Avp*) mRNA levels were lower in the SCN of Tg(Fgf21) mice compared to wild-type mice (Fig. 2d). Importantly, intracerebroventricular (i.c.v.) administration of either kisspeptin or vasopressin to Tg(Fgf21) mice was sufficient to restore the ability of the hypothalamus to induce an LH surge (Fig. 2e,f). Together, these data demonstrate that FGF21 perturbs the hypothalamic neuroendocrine axis that is essential for ovulation. Our finding that FGF21 affects AVPV

kisspeptin neurons without affecting the Arc population provides a possible explanation for the lack of effect of FGF21 on male fertility, since male mice are virtually devoid of kisspeptin neurons in the AVPV[21].

β-Klotho is an essential co-receptor for FGF21 (ref. [22]), and in the forebrain *Klb* expression is restricted to the SCN (Bookout *et. al.* accompanying paper). To examine the requirement of the forebrain for the reproductive effects of FGF21, we crossed the Tg(Fgf21) into homozygous *Klb*-floxed mice (Klb^{tm1}) expressing cre-recombinase from the calcium/calmodulin-dependent kinase IIa (*Camk2a*) promoter. This strategy creates a mouse strain ($Klb^{tm1(Camk2a)}$) that selectively eliminates *Klb* expression in the SCN of Tg(Fgf21) mice (Bookout *et. al.*). Notably, the deletion of *Klb* in the forebrain of female Tg(Fgf21) mice resulted in higher expression of *Kiss1* in the AVPV and *Avp* in the SCN compared to Klb^{tm1} control mice (Fig. 3a). Estrous cycles were restored in 13 out of 14 $Klb^{tm1(Camk2a)}$::Tg(Fgf21) mice (Fig. 3b). Furthermore, all of the $Klb^{tm1(Camk2a)}$::Tg(Fgf21) mice became pregnant after mating with stud males (Fig. 3c). As shown in the companion paper (Bookout *et al.*), *Klb* is also expressed in the dorsal vagal complex of the hindbrain. Eliminating *Klb* in the hindbrain using a *Phox2b*-cre mouse line (Bookout *et al.*) did not restore estrus in any of the female mice (Supplementary Fig. 2). These results show that β-Klotho-mediated FGF21 signaling in the forebrain leads to an abnormal gonadotropic response to estradiol and anovulation.

Multiple, redundant, mechanisms have evolved to prevent pregnancy during nutritional deprivation[1–7]. We aimed to determine whether FGF21 contributes to this important adaptive process. First, we tested whether $Klb^{tm1(Camk2a)}$ mice are resistant to fasting-induced infertility. Whereas fasting (48 h) perturbed the estrous cycle in all mice, the delay in ovulation upon re-feeding was significantly shorter in $Klb^{tm1(Camk2a)}$ compared to Klb^{tm1} mice (Fig. 4a). In addition, the expression of *Kiss1* in the AVPV and *Avp* in the SCN was significantly higher in $Klb^{tm1(Camk2a)}$ mice than in Klb^{tm1} mice following a 48 h fast (Fig. 4b). The finding that β-Klotho in the SCN is required for the normal reproductive response to starvation in female mice strongly supports the notion of a physiologic FGF21-neuroendocrine axis.

Finally, we used subcutaneous osmotic mini-pumps to assess the effect of longer-term exposure to fasting levels of FGF21 on female reproduction. Continuous infusion of recombinant human FGF21 at a rate of 1.1 μg h^{-1} resulted in stable plasma levels between 5 and 10 ng ml^{-1} (Fig. 4c), which are similar to physiologic levels achieved during fasting (Ref. [23] and Bookout *et. al.* accompanying paper). There was no effect of FGF21 at these concentrations on body weight, body composition or plasma leptin levels (Supplementary Fig. 3). However, this treatment was sufficient to terminate estrous cycles in five out of six female Klb^{tm1} mice (Fig. 4d). By contrast, estrous cycles were maintained in FGF21-treated $Klb^{tm1(Camk2a)}$ mice (Fig. 4d). Similarly, *Kiss1* expression in the AVPV and *Avp* expression in the SCN were decreased by FGF21 in an SCN-*Klb*-dependent manner (Fig. 4e). Together, these findings demonstrate that exposure to fasting levels of FGF21 is sufficient to cause female infertility in adult mice, and that β-Klotho-dependent FGF21 signaling in the SCN may contribute to suppressing female fertility as part of the adaptive starvation response.

In summary, these studies define a liver-neuroendocrine signaling pathway in which FGF21, acting through the SCN in the hypothalamus, contributes to the suppression of ovulation during starvation (Fig. 4f). In an accompanying paper (Bookout *et al.*), we show that FGF21 action on the hypothalamus also increases corticosterone levels, suppresses growth, and alters behavior. While the effects of FGF21 on metabolic parameters, including plasma insulin and glucocorticoid concentrations, may also contribute to the female infertility, our finding that direct i.c.v. injection of either vasopressin or kisspeptin into female Tg(Fgf21) mice rapidly induced an LH surge indicates that FGF21 causes infertility in part by dampening the output of the SCN, which in turn governs the kisspeptin-GnRH-LH neuroendocrine circuit (Fig. 4f). Notably, SCN-derived vasopressin is part of the neuroendocrine pathway that also suppresses corticosterone secretion from the adrenal [24]. Thus, the suppression of vasopressin expression in the SCN may be the mechanism unifying the effects of FGF21 on circulating glucocorticoid levels, female reproduction, and possibly other physiologic processes. Finally, the observation that FGF21 can also be elevated systemically by obesity[25], suggests that FGF21 might contribute to the reproductive anomalies that have been associated with the metabolic syndrome[26].

Online Methods

Animals

All procedures and use of animals were approved by the Institutional Animal Care and Use Committee of UT Southwestern Medical Center Dallas. The C57BL/6J Tg(Fgf21), C57BL/6J *Fgf21*$^{-/-}$, C57BL/6J;129/Sv *Klb*^{tm1}, and C57BL/6J *Camk2a*-cre lines have been previously described [9,13,22,27]. All mice were age matched, housed under phytoestrogen-free conditions and, unless otherwise stated, single caged during experimentation. Standard chow was from Harlan Teklad Diets (#2916; Madison, WI). For mini-pump experiments, Alzet micro-osmotic pumps were filled with vehicle or recombinant FGF21 and implanted subcutaneously under inhalation anaesthesia. Animals were sacrificed by decapitation at ZT3, 7-days after implantation.

Reagents and Materials

Estradiol (17β-estradiol), estradiol benzoate, vasopressin acetate salt, gonadotropin from pregnant mare serum (PMSG), Leuprolide acetate salt, 0.9% sodium chloride solution and sesame oil were from Sigma-Aldrich, Co (St Louis, MO). Kisspeptin (110–119) amide was from Phoenix Pharmaceuticals (Burlingame, CA). Generation of recombinant human FGF21 has been described previously [13]. Artificial cerebrospinal fluid was from Harvard Apparatus (Hollsont, MA). Alzet micro-osmotic pumps were from DURECT Corporation (Cupertino, CA). Silastic laboratory tubing was from Dow Corning Corporation (Midland, MI). Brain guide cannulae and injection catheters were from PlasticsOne (Roanoke, VA).

Hormone analysis

Plasma FSH and LH analysis were performed by the University of Virginia Center for Research in Reproduction. ELISA kits were used to determine levels of circulating estradiol (Alpco, Salem, NH), leptin (Millipore, Billerica, MA) and FGF21 (BioVendor, Czech Republic).

Assessment of estrous cycles and fertility

The stage of the estrous cycle was determined by vaginal cytology, essentially as described [28]. The age at onset of puberty was determined by the day of vaginal opening and/or the day of first estrus. Reproductive competency was determined by the proportion of experimental females that mated (evidence of a vaginal plug, uterine implantations sites or overt pregnancy) with proven stud males over a defined time period (typically 3–4 weeks).

Ovarian transplantations

Wild-type littermates served as recipients for ovaries from Tg(Fgf21) mice. Following removal of wild-type ovaries and implantation of Tg(Fgf21) ovaries, mice were allowed to recover for one week and were then mated with wild-type males. Pregnant animals were sacrificed at E14. Ovaries of pregnant animals were bisected to allow both histological examination of corpora lutea and genotyping for the presence of the Fgf21-transgene. Confirmation of successful ovarian transplant and function was based on the presence of the Fgf21-transgene in the ovary and in at least one fetus.

Estrogen surge experiment

Mice received a single intraperitoneal injection of vehicle (saline) or PMSG (0.2 IU g^{-1}) at ZT7 on the first day of the follicular phase of the cycle. Blood was collected for estradiol measurement 24 h post-injection.

LH surge experiments

A standard protocol was followed to induce an estrogen-stimulated LH surge [29]. Briefly, mice were ovariectomized and implanted with a Silastic pellet containing estradiol (1 cm pellet containing 0.1 mg ml^{-1} 17β-estradiol in sesame oil). Animals were allowed to recover for one week and then received an intaperitoneal injection of estradiol benzoate (0.05 mg kg^{-1}) or vehicle (sesame oil) at ZT2. Blood was collected for LH measurement at ZT13.5 the following day.

The ability of leuprolide to stimulate pituitary LH secretion was tested in wild-type and Tg(Fgf21) mice. Animals were ovariectomized and implanted with a Silastic pellet containing estradiol (as above). The mice were allowed to recover for one week and then received an intaperitoneal injection of vehicle (saline) or leuprolide (1μg/kg) at ZT9. Blood was collected for LH measurement 1h post-injection.

The ability of kisspeptin to induce an LH surge was tested in intact Tg(Fgf21) mice. Animals underwent surgery for the implantation of a guide cannula (co-ordinates from the bregma: AP −0.34 mm, L/R +1 mm, D −2.3 mm). Following recovery for one week, mice received a single i.c.v. injection of vehicle (artificial cerebral spinal fluid) or kisspeptin (1 nM in 1 μl volume) at ZT9. Blood was collected for LH measurement 1 h post-injection.

The ability of vasopressin to rescue an estrogen-stimulated LH surge was tested in Tg(Fgf21) mice. Animals underwent guide cannula surgery, ovariectomy, Silastic pellet implantation and estradiol benzoate injection as described above. A single i.c.v. injection of vehicle (artificial cerebral spinal fluid) or vasopressin (3 ng in 1.5 μl) was administered at

ZT6 on the day after estradiol injection and blood was collected at ZT13 for LH measurement.

Brain dissection

The brain was rapidly removed from the skull and placed on ice. Punches from the AVPV, SCN, and arcuate nucleus of the hypothalamus were cut away from the surrounding tissue of 0.5 mm-thick coronal slices under RNAse-free conditions. Care was taken to avoid adjacent nuclei. The location of nuclei was determined in relation to white matter landmarks (anterior commissure and optic chiasm) and the third ventricle, with the aid of the Paxinos Mouse Brain Atlas.

Gene expression analysis

Standard protocols were followed for quantifying gene expression of mouse tissue. Primers for detecting *Fgf21*, *Kiss1* and *Avp* mRNA are available upon request.

Statistics

Data are presented as mean ± SEM. Two-tailed Student's *t*-test. $P < 0.05$ was considered significant.

Supplementary Material

Refer to Web version on PubMed Central for supplementary material.

Acknowledgments

We thank R. Hammer and members of the Mangelsdorf/Kliewer laboratory for discussion; Y. Zhang, H. Lawrence, and L. Harris for technical assistance; J. Shelton for imaging; R. Goetz and M. Mohammadi for FGF21 protein. This research was supported by the Howard Hughes Medical Institute (D.J.M.), NIH grants RL1GM084436 and R56DK089600 (D.J.M. and S.A.K.), U19DK62434 (D.J.M), and GM007062 (A.L.B.), the Robert A. Welch Foundation (I-1275 to D.J.M. and I-1558 to S.A.K.). The University of Virginia Center for Research in Reproduction Ligand Assay and Analysis Core is supported by the Eunice Kennedy Shriver NICHD/NIH (SCCPIR) Grant U54-HD28934.

References

1. Burks DJ, et al. IRS-2 pathways integrate female reproduction and energy homeostasis. Nature. 2000; 407:377–382. [PubMed: 11014193]
2. Chehab FF, Lim ME, Lu R. Correction of the sterility defect in homozygous obese female mice by treatment with the human recombinant leptin. Nature Genetics. 1996; 12:318–320. [PubMed: 8589726]
3. Della Torre S, et al. Amino acid-dependent activation of liver estrogen receptor alpha integrates metabolic and reproductive functions via IGF-1. Cell Metabolism. 13:205–214. [PubMed: 21284987]
4. Altarejos JY, et al. The Creb1 coactivator Crtc1 is required for energy balance and fertility. Nature Medicine. 2008; 14:1112–1117.
5. Kalamatianos T, Grimshaw SE, Poorun R, Hahn JD, Coen CW. Fasting reduces KiSS-1 expression in the anteroventral periventricular nucleus (AVPV): effects of fasting on the expression of KiSS-1 and neuropeptide Y in the AVPV or arcuate nucleus of female rats. Journal of Neuroendocrinology. 2008; 20:1089–1097. [PubMed: 18573184]

6. Roa J, et al. The mammalian target of rapamycin as novel central regulator of puberty onset via modulation of hypothalamic Kiss1 system. Endocrinology. 2009; 150:5016–5026. [PubMed: 19734277]
7. Bruning JC, et al. Role of brain insulin receptor in control of body weight and reproduction. Science. 2000; 289:2122–2125. [PubMed: 11000114]
8. Goetz R, et al. Molecular insights into the -Klotho-dependent, endocrine mode of action of fibroblast growth factor 19 subfamily members. Molecular and Cellular Biology. 2007; 27:3417–3428. [PubMed: 17339340]
9. Inagaki T, et al. Endocrine regulation of the fasting response by PPARalpha-mediated induction of fibroblast growth factor 21. Cell Metabolism. 2007; 5:415–425. [PubMed: 17550777]
10. Galman C, et al. The circulating metabolic regulator FGF21 is induced by prolonged fasting and PPARalpha activation in man. Cell Metabolism. 2008; 8:169–174. [PubMed: 18680716]
11. Hondares E, et al. Hepatic FGF21 expression is induced at birth via PPARalpha in response to milk intake and contributes to thermogenic activation of neonatal brown fat. Cell Metabolism. 11:206–212. [PubMed: 20197053]
12. Kharitonenkov A, et al. FGF-21 as a novel metabolic regulator. The Journal of Clinical Investigation. 2005; 115:1627–1635. [PubMed: 15902306]
13. Potthoff MJ, et al. FGF21 induces PGC-1alpha and regulates carbohydrate and fatty acid metabolism during the adaptive starvation response. Proceedings of the National Academy of Sciences of the United States of America. 2009; 106:10853–10858. [PubMed: 19541642]
14. Potthoff MJ, Kliewer SA, Mangelsdorf DJ. Endocrine fibroblast growth factors 15/19 and 21: from feast to famine. Genes & Development. 26:312–324. [PubMed: 22302876]
15. Zhang Y, et al. The starvation hormone, fibroblast growth factor-21, extends lifespan in mice. Elife. 1:e00065. [PubMed: 23066506]
16. Roa J, Navarro VM, Tena-Sempere M. Kisspeptins in reproductive biology: consensus knowledge and recent developments. Biology of Reproduction. 85:650–660. [PubMed: 21677307]
17. Mayer C, et al. Timing and completion of puberty in female mice depend on estrogen receptor alpha-signaling in kisspeptin neurons. Proceedings of the National Academy of Sciences of the United States of America. 107:22693–22698. [PubMed: 21149719]
18. Miller BH, et al. Vasopressin regulation of the proestrous luteinizing hormone surge in wild-type and Clock mutant mice. Biology of Reproduction. 2006; 75:778–784. [PubMed: 16870944]
19. Vida B, et al. Evidence for suprachiasmatic vasopressin neurones innervating kisspeptin neurones in the rostral periventricular area of the mouse brain: regulation by oestrogen. Journal of Neuroendocrinology. 22:1032–1039. [PubMed: 20584108]
20. Roa J, et al. Kisspeptins and the control of gonadotropin secretion in male and female rodents. Peptides. 2009; 30:57–66. [PubMed: 18793689]
21. Clarkson J, Herbison AE. Postnatal development of kisspeptin neurons in mouse hypothalamus; sexual dimorphism and projections to gonadotropin-releasing hormone neurons. Endocrinology. 2006; 147:5817–5825. [PubMed: 16959837]
22. Ding X, et al. beta-Klotho Is Required for Fibroblast Growth Factor 21 Effects on Growth and Metabolism. Cell Metabolism. 16:387–393. [PubMed: 22958921]
23. Inagaki T, et al. Inhibition of growth hormone signaling by the fasting-induced hormone FGF21. Cell Metabolism. 2008; 8:77–83. [PubMed: 18585098]
24. Kalsbeek A, Buijs RM, van Heerikhuize JJ, Arts M, van der Woude TP. Vasopressin-containing neurons of the suprachiasmatic nuclei inhibit corticosterone release. Brain Research. 1992; 580:62–67. [PubMed: 1504818]
25. Woo YC, Xu A, Wang Y, Lam KS. Fibroblast growth factor 21 as an emerging metabolic regulator: clinical perspectives. Clinical Endocrinology (Oxf). 78:489–496.
26. Cardozo E, Pavone ME, Hirshfeld-Cytron JE. Metabolic syndrome and oocyte quality. Trends in Endocrinology and Metabolism. 22:103–109. [PubMed: 21277789]

Online Methods References

27. Casanova E, et al. A CamKIIalpha iCre BAC allows brain-specific gene inactivation. Genesis. 2001; 31:37–42. [PubMed: 11668676]
28. Caligioni CS. Assessing reproductive status/stages in mice. Current Protocols in Neuroscience. 2009 Appendix 4, Appendix 4I.
29. Quennell JH, et al. Leptin deficiency and diet-induced obesity reduce hypothalamic kisspeptin expression in mice. Endocrinology. 152:1541–1550. [PubMed: 21325051]

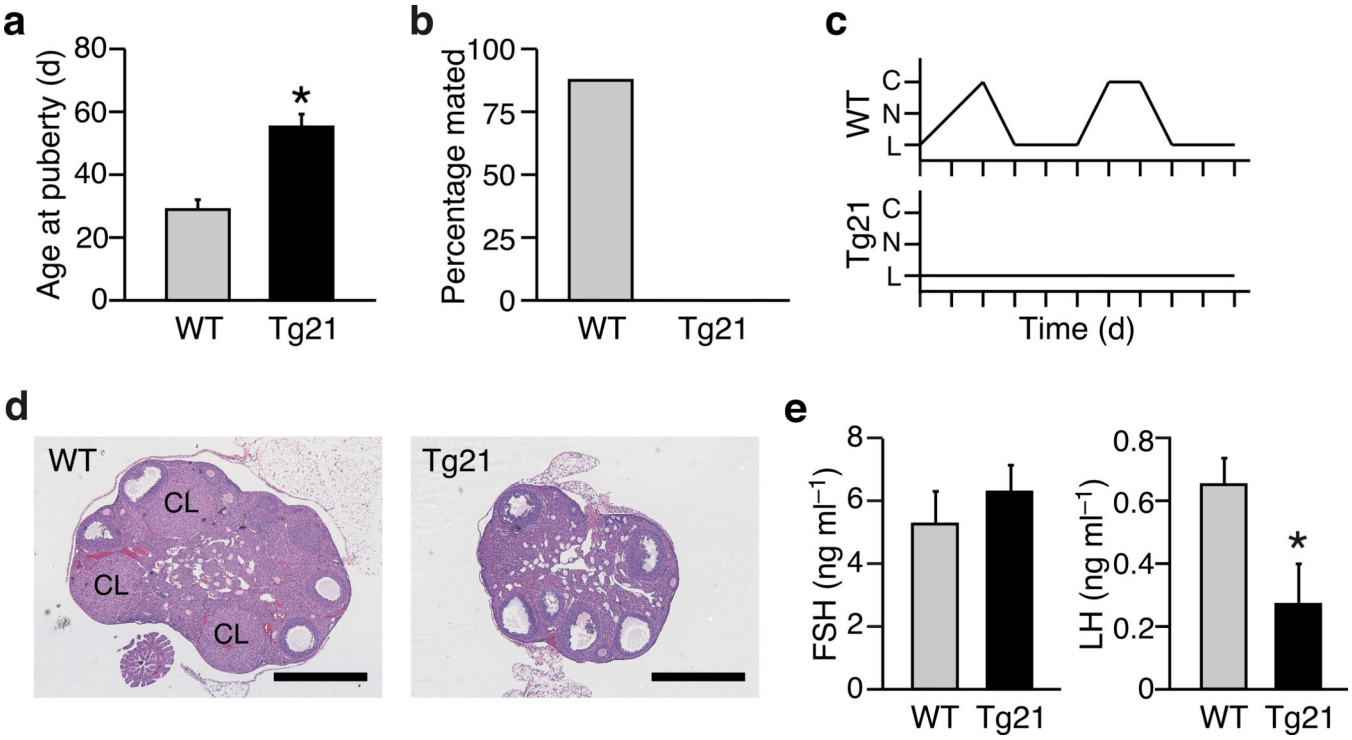

Figure 1.

Female Tg(Fgf21) mice are infertile. (**a**) Age at onset of puberty (vaginal opening) in female wild-type (WT) and Tg(Fgf21) (Tg21) mice (n = 6–7). (**b**) Proportion of WT and Tg(Fgf21) mice that mated with proven stud males (n = 8). (**c**) Representative examples of estrus cycles in WT and Tg(Fgf21) mice as determined by vaginal cytology (C: cornified cells [estrus], N: nucleated cells [proestrus], L: leukocytes [diestrus]). (**d**) Examples of ovarian histology from WT and Tg(Fgf21) mice (CL: corpora lutea). Bar = 500 μm. (**e**) Plasma FSH and LH levels measured in diestrus at ZT6–7 (n = 5). Data represent the mean ± SEM, *P < 0.05 compared to WT.

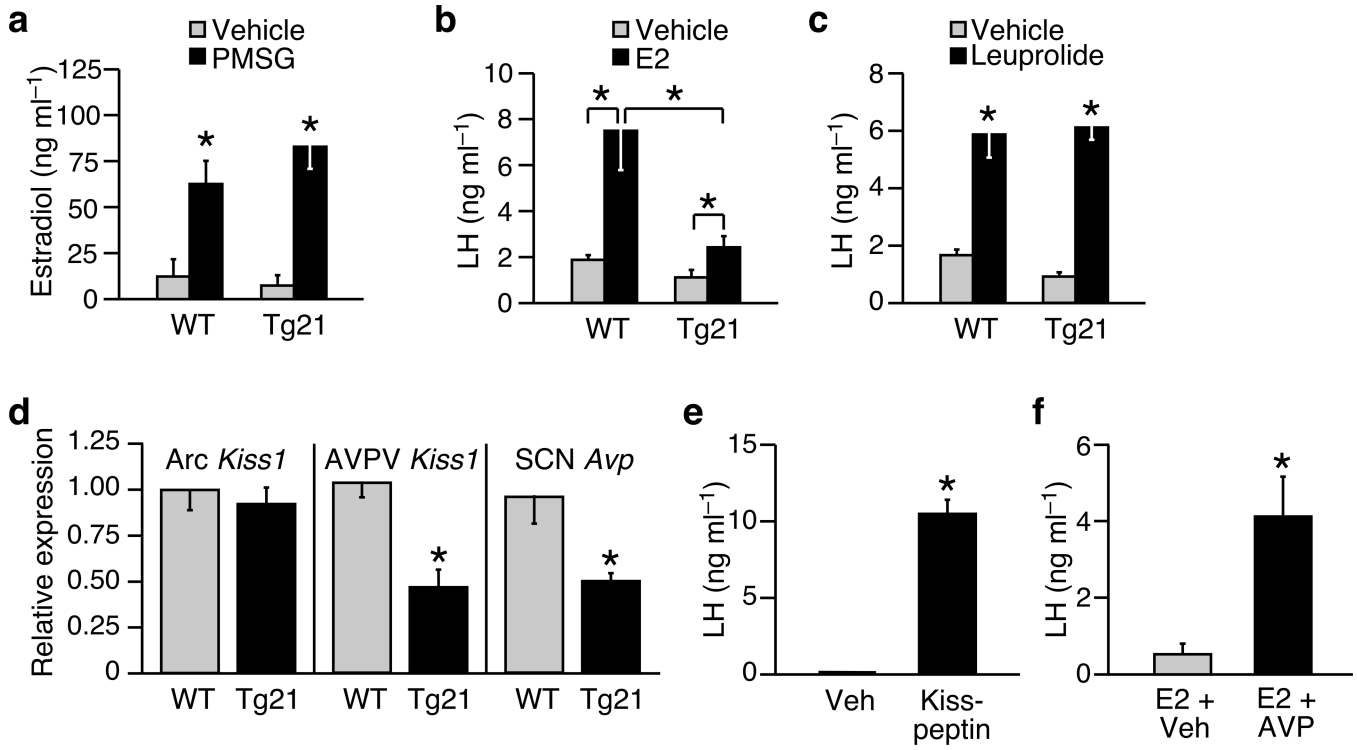

Figure 2.

Female Tg(Fgf21) mice display hypothalamic hypogonadism. (**a**) Plasma estradiol levels in (wild-type) WT and Tg(Fgf21) (Tg21) mice (n = 7–9) treated with saline or gonadotropin from pregnant mare serum (PMSG). (**b, c**) Plasma LH in WT and Tg(Fgf21) mice (n = 4–6) treated with vehicle and estradiol (E2) or vehicle and the GnRH-receptor agonist leuprolide. (**d**) *Kiss1* expression in the arcuate (Arc) and anteroventral periventricular (AVPV) nuclei, or vasopressin (*Avp*) expression in the suprachiasmatic nucleus (SCN) of female WT and Tg(Fgf21) mice in diestrus (n = 8). (**e**) Plasma LH in Tg(Fgf21) mice treated with a single i.c.v injection of vehicle (artificial cerebral spinal fluid) or kisspeptin (n = 4). (**f**) Plasma LH in Tg(Fgf21) mice (n = 4–6) treated with estradiol (E2) and an i.c.v injection of either vehicle (artificial cerebral spinal fluid) or vasopressin (AVP). Data represent the mean ± SEM; *P < 0.05 compared to Veh or WT controls, or as indicated in figure.

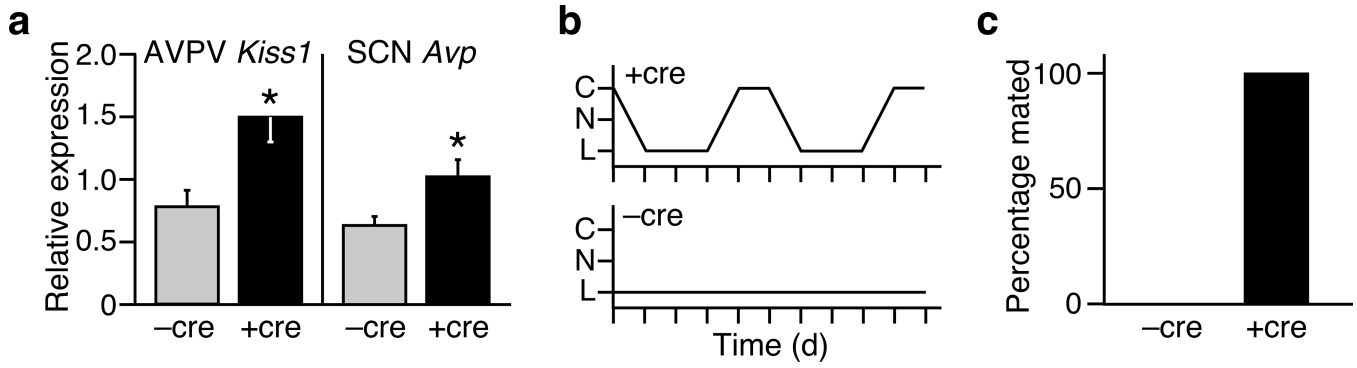

Figure 3.

Klb expression in the hypothalamus is essential for FGF21-mediated effects on ovulation. (**a**) Hypothalamic gene expression in *Klb*^{tm1}::Tg(Fgf21) mice in the presence (+ cre) or absence (−cre) of *Camk2a*-Cre (n = 7–8). (**b, c**) Representative examples of estrus cycles and quantification of mating success in *Klb*^{tm1}::Tg(Fgf21) mice in the presence (n = 14) or absence (n = 6) of *Camk2a*-Cre. Data represent the mean ± SEM; *P < 0.05 compared to −cre controls.

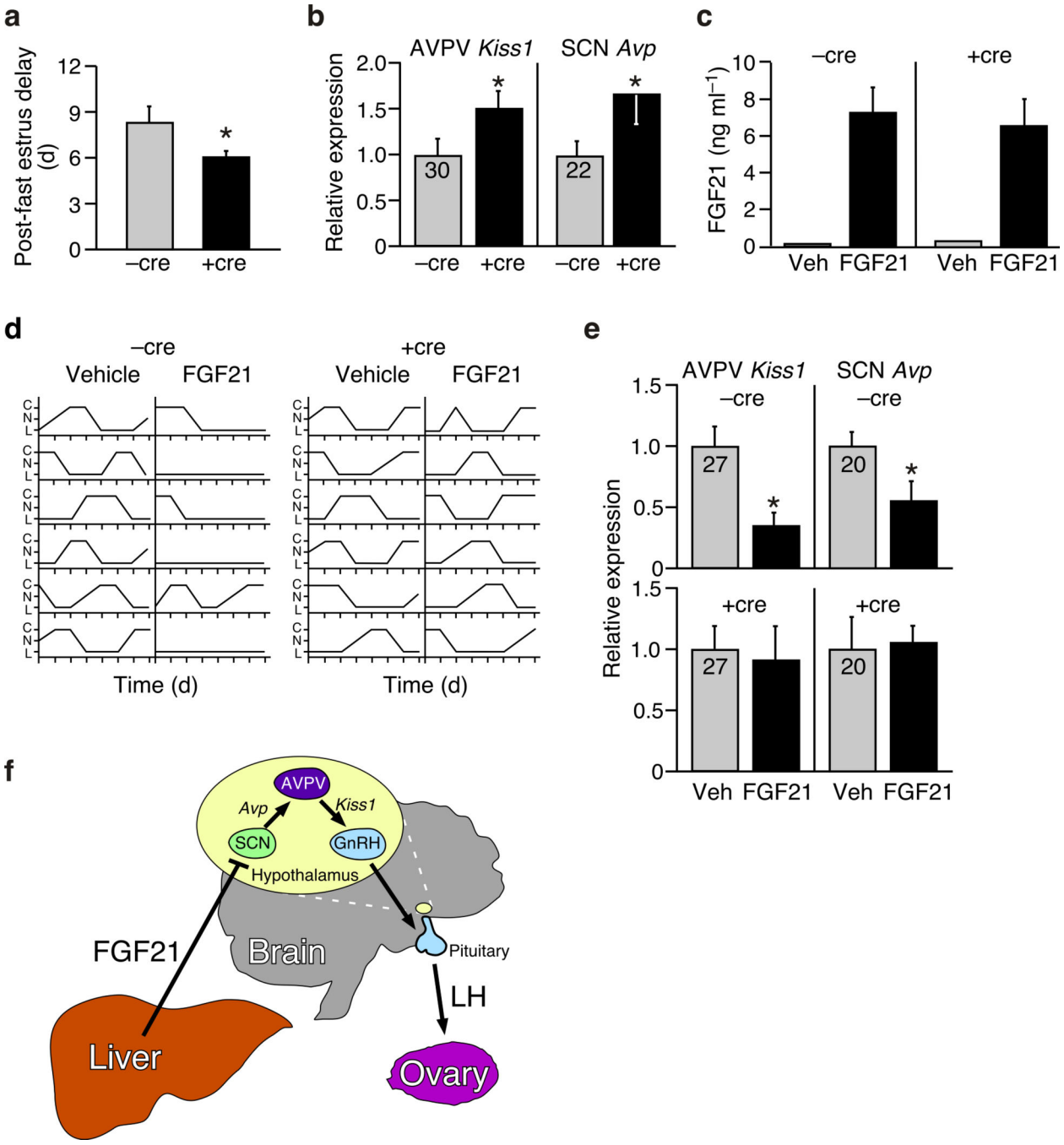

Figure 4.

Evidence that FGF21 modulates female reproduction as part of the adaptive starvation response. (**a**) Delayed ovulation caused by a 48 h fast in *Klb*^{tm1} (−cre) and *Klb*$^{tm1(Camk2a)}$ (+cre) mice (n = 6). (**b**) Hypothalamic gene expression in in *Klb*^{tm1} (−cre) and *Klb*$^{tm1(Camk2a)}$ (+cre) mice following a 48 h fast (n = 6). Cycle time (Ct) values are shown for −cre controls. (**c**) Plasma human FGF21 levels achieved by osmotic mini-pump infusion of vehicle (V) or hFGF21 (n = 6). (**d**) Effects of mini-pump administration of FGF21 on estrus cycles and (**e**) hypothalamic gene expression in in *Klb*^{tm1} (−cre) and *Klb*$^{tm1(Camk2a)}$

(+cre) mice (n = 6). Ct values are shown for vehicle (veh) controls. (**f**) Model of FGF21 action on the hypothalamic-pituitary-ovarian axis. Data represent the mean ± SEM; *P < 0.05 compared to −cre controls.